Journal of Biomechanics 46 (2013) 77–82

Contents lists available at SciVerse ScienceDirect

Journal of Biomechanics

journal homepage: www.elsevier.com/locate/jbiomech
www.JBiomech.com

Spring-like gait mechanics observed during walking in both young and older adults

Hyunhwa Hong [a], Seyoung Kim [b], Cheolwoong Kim [c,d], Soonhyuck Lee [e,1], Sukyung Park [a,*,1]

[a] Department of Mechanical Engineering, Korea Advanced Institute of Science and Technology (KAIST), Daejeon, Republic of Korea
[b] Korea Institute of Machinery and Materials (KIMM), Daejeon, Republic of Korea
[c] Institute of Technology and Engineering (RITE), Korea University, Seoul, Republic of Korea
[d] Triple-C Medical Corporation, Seoul, Republic of Korea
[e] Department of Orthopedic Surgery, Korea University, Seoul, Republic of Korea

ARTICLE INFO

Article history:
Accepted 4 October 2012

Keywords:
Older adults
Walking
Leg stiffness
Gait speed

ABSTRACT

A spring loaded inverted pendulum model successfully demonstrated the oscillatory behavior of the center of mass (CoM) and corresponding ground reaction forces (GRFs) of young healthy subjects. This study questioned whether spring-like leg walking dynamics are consistently observed in the walking of older adults that exhibit different gait characteristics, such as slower gait speed, from the young. Eight young and eight older adult subjects participated in overground walking experiments performed at four different gait speeds, ranging from their self-selected speed to a maximum walking speed. To calculate the effective leg stiffness, the damped compliant leg model with a curved foot was used. The model parameters of leg stiffness and damping constant were optimized to achieve the best fit between model and human GRFs data. We observed that the GRFs data from both age groups were reasonably well fitted by spring-like leg dynamics throughout the broad range of gait speeds. The leg stiffness and damping constant consistently increased as a function of the walking speed in both age groups, but slightly greater variations of the model parameters were observed for the older adults' trials. The results imply that human walking dynamics and the variation with respect to age can be well captured by spring-like leg dynamics.

© 2012 Elsevier Ltd. All rights reserved.

1. Introduction

One of the mechanical factors that has been used to describe gait mechanics is stiffness, which is defined as the ratio of the applied force to the corresponding deformation (Davis and DeLuca, 1996; Farley and Gonzalez, 1996; Holt et al., 2003; Rebula et al., 2009). The ankle or knee joint stiffness, which represents the joint resistance by the passive tissues as well as active muscle contraction, is defined as the ratio of the joint moment change with respect to the joint excursion and is used to quantify the changes in gait characteristics due to disease (Hunter and Kearney, 1982; Davis and DeLuca, 1996; Zeni and Higginson, 2009) or loading conditions (Holt et al., 2003). In addition to the joint mechanics point of view, the oscillatory movement of the body's center of mass (CoM) and the corresponding ground reaction forces (GRFs) are related to a type of global stiffness (Holt et al., 1995,2003) or vertical stiffness (Holt et al., 2000, 2003; Fonseca et al., 2001; Lipfert et al., 2005; Rebula et al., 2009). The global stiffness of the compliant leg has been estimated from the gait period when the CoM excursion during walking is assumed to be a harmonic oscillator response that includes the body mass on a compliant leg pivoted at the ankle joint (Holt et al., 1995,2003). The vertical stiffness is defined as the ratio of the changes in vertical GRF and the corresponding vertical CoM motion and has been used to describe the changes in speed-dependent gait dynamics (Holt et al., 2003; Lipfert et al., 2005; Rebula et al., 2009). However, the stiffness profiles obtained from the instantaneous derivative of the force with respect to the CoM motion showed temporal variations and are limited in their ability to represent the gait dynamics over a complete gait cycle as a single system variable. Therefore, to obtain the representative stiffness estimate during the specific gait phase of interest, averaging of the stiffness profiles has been performed over a complete or a specific gait cycle (Davis and DeLuca, 1996; Holt et al., 2003; Lark et al., 2003; Lipfert et al., 2005; Rebula et al., 2009; Zeni and Higginson, 2009).

To describe the kinetics of a complete gait cycle in terms of a single stiffness parameter, a simple bipedal gait model with a compliant leg has been proposed by Geyer et al. (Geyer et al., 2006). The springy bipedal model demonstrated the shared

* Correspondence to: Department of Mechanical Engineering, Korea Advanced Institute of Science and Technology (KAIST), 335 Gwahangno, Yuseong-gu, Daejeon 305-701, Republic of Korea. Tel.: +82 42 350 3230; fax: +82 42 350 5230.
E-mail address: sukyungp@kaist.ac.kr (S. Park).
[1] These authors contributed equally to this work.

0021-9290/$ - see front matter © 2012 Elsevier Ltd. All rights reserved.
http://dx.doi.org/10.1016/j.jbiomech.2012.10.003

mechanics of human walking and running, which have often been treated as two different mechanical systems in previous studies (Alexander, 1976; Mochon and McMahon, 1980; Blickhan, 1989; McMahon and Cheng, 1990). Inspired by the compliant leg bipedal modeling studies (Geyer et al., 2006; Srinivasan and Ruina, 2006; Whittington and Thelen, 2009), Kim and Park quantified the gait dynamics in terms of the model parameters of a mass-spring-damper system that best matched the temporal profiles of the GRFs and the CoM (Kim and Park, 2011). A velocity-dependent increase in the leg stiffness parameter was observed to be closely correlated with the system's natural frequency and a mechanical benefit of human walking using spring-like leg mechanics (Kim and Park, 2011). Previous attempts to describe the gait response of healthy young adults in terms of the mechanics of a mass-spring system led to the question of whether the spring-like leg dynamics of walking would be consistently observed in the walking of older adults, known to have different gait characteristics, such as slower gait speed (Imms and Edholm, 1981; Himann et al., 1988; Elble et al., 1991; Wall et al., 1991; Dobbs et al., 1993), shortened step length (Murray et al., 1969; Larish et al., 1988; Winter et al., 1990), and reduced GRFs (Winter, 1991; Eng and Winter, 1995), compared with the young. Therefore, in this study, the possibility of describing the gait dynamics of the older adults by spring-like like leg dynamics was investigated. The speed-dependent changes of the model parameters of the older adults are also compared to those of the younger subjects. Empirical data were collected and analyzed using a damped compliant leg model with a curved foot.

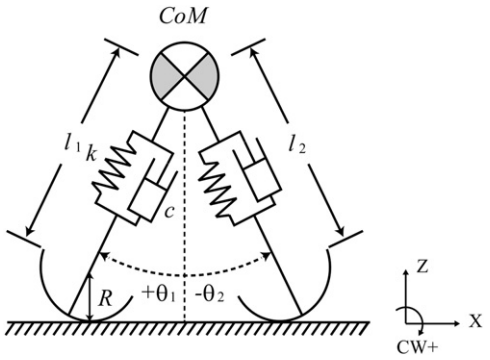

Fig. 1. Schematic of a damped compliant walking model. The model parameters m, k, and c are the body mass, spring constant, and damping constant, respectively. The leg angle, θ, and leg length, L, were obtained by solving the equations of motion. The leg stiffness, k, and the damping constant, c, are optimization parameters obtained from the data fitting. The radius of the curved foot, R, was set to 0.3. Subscripts '1' and '2' indicate the trailing leg and the leading leg, respectively.

2. Methods

2.1. Subjects

Eight young (7M/1F, 23.5 ± 1.77 yr, mean ± S.D.) and eight healthy older adult (5M/3F, 67.9 ± 2.53 yr) subjects were recruited from the local community. All subjects had no history of balance disorders and did not experience discomfort while walking. The study was performed in accordance with the IRB, and ethical approval for the procedures was obtained from the Korea Advanced Institute of Science and Technology. Detailed explanations of the experimental methods were

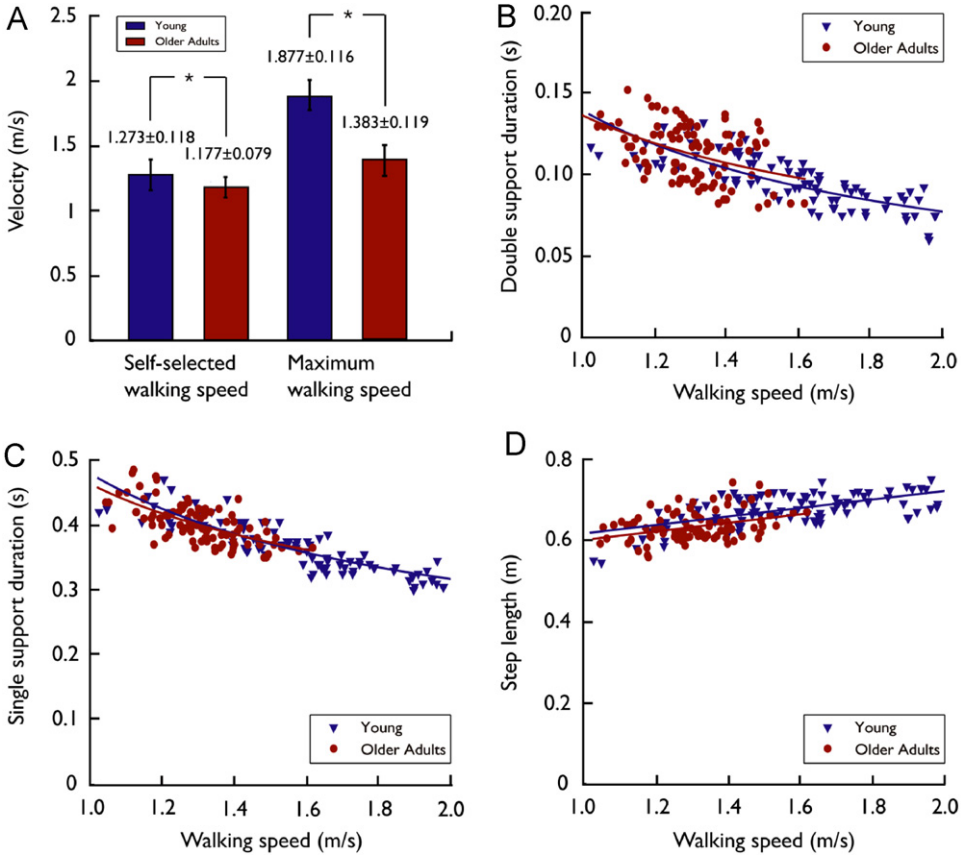

Fig. 2. The empirical data of the gait parameters for the young (blue-colored reversed triangle, ▲) and the older adults (red-colored circle, ●). Consistent marker codes were used throughout the paper. (A) The average of the natural and the maximum walking speed of both age groups. (B) The double- and (C) the single-support duration and (D) the step length as a function of speed, which ranged from a self-selected to a maximum walking speed. The solid lines indicate the curve fit of the data. The regression parameters are shown in Table 2. (For interpretation of the references to color in this figure legend, the reader is referred to the web version of this article.)

provided to the subjects, and all subjects signed informed consent forms prior to testing. The average height and weight of the young and older subject groups were 1.68 ± 0.06 m (mean $\pm$ S.D.) and 66.75 ± 10.74 kg and 1.61 ± 0.08 m and 64.00 ± 14.16 kg, respectively.

2.2. Protocols

The subjects walked on a 12-m long and 1-m wide walkway for three blocks at four different gait speeds controlled by stepping to a metronome at different frequencies. Prior to data collection, we measured each subject's natural and maximum gait speeds and the associated step frequencies and subsequently set the gait frequency interval to one-third of the difference between the gait frequencies of the natural and maximum walking speeds for each subject. The subjects were verbally instructed to initiate their gait and to walk in accordance with an auditory cue offered by the metronome (Dual Metronome Reference Pitch Generator SMT-1000, SAMICK®) corresponding to each gait frequency. We measured the GRFs of three consecutive steps after 5–6 steps of gait initiation, which were performed to reach steady-state walking. To avoid intentional stepping on the platform during walking, the force platform was covered with a thin carpet. Trials were discarded if the subject did not perform a steady-state gait or if the steps were not completely on the force platform. Between each set of 4 trials, the subjects took a 5-min break. The details of the experimental procedure have been presented previously (Yeom and Park, 2011).

2.3. Measurement

The kinetic and kinematic data were collected using three force plates (AMTI, Accugait®) and motion capture cameras (Motion Analysis, Hawk®) using a 200 Hz sampling frequency. Optical markers were attached to the sacrum (L5), left lateral malleolus, and right lateral malleolus and were used to calculate the leg configurations. Ground reaction forces were integrated to obtain the velocity and the position of the CoM (Gard et al., 2004), with the sacral marker used for determining the integral constant. The optical marker positions and the GRFs were filtered using a 5th-order Butterworth low-pass filter with cutoff frequencies of 10 Hz and 30 Hz, respectively.

2.4. Model analysis and simulation

To calculate the mechanical parameters of gait dynamics as a function of walking speed, we used a compliant, damped bipedal walking model (Fig. 1) that is similar to that used in a previous study (Kim and Park, 2011). The model consisted of a point body mass (M) that represents the whole body mass, two massless compliant legs of stiffness, k, damping constant, c, and massless curved feet of radius, R. The stiffness component generates the oscillatory behavior of the CoM during the gait cycle and the damper restrains the leg from excessive CoM excursions. Both the stiffness and the damping constant were assumed to be constant during the gait cycle. A curved foot emulates the center of pressure (CoP), and a non-slip condition at the contact point between the curved foot and the ground was assumed.

The equations of motion for the model were obtained using Lagrange's method as follows:

$$\begin{bmatrix} MR\sin\theta_1 & M \\ Ml_1^2+2MRl_1\cos\theta_1+MR^2 & MR\sin\theta_1 \end{bmatrix} \begin{bmatrix} \ddot{\theta}_1 \\ \ddot{l}_1 \end{bmatrix} = \begin{bmatrix} -MR\dot{\theta}_1^2\cos\theta_1+Ml_1\dot{\theta}_1^2+MR\dot{\theta}_1^2\cos\theta_1-Mg\cos\theta_1+Kl_0-Kl_1 \\ +(Kl_0-Kl_2)\left(\frac{l_2\cos(\theta_1-\theta_2)+R\cos\theta_1}{l_2+R\cos\theta_2}\right)-C\dot{l}_1-C\dot{l}_2\left(\frac{l_2\cos(\theta_1-\theta_2)+R\cos\theta_1}{l_2+R\cos\theta_2}\right) \\ -2Ml_1\dot{l}_1\dot{\theta}_1-3MR\dot{l}_1\dot{\theta}_1\cos\theta_1+MRl_1\dot{\theta}_1^2\sin\theta_1+MR\dot{l}_1\dot{\theta}_1\cos\theta_1+Mgl_1\sin\theta_1 \\ +(Kl_0-Kl_2)\left(\frac{Rl_2\sin\theta_2-l_1l_2\sin(\theta_1-\theta_2)-Rl_1\sin\theta_1}{l_2+R\cos\theta_2}\right)-C\dot{l}_2\left(\frac{Rl_2\sin\theta_2-l_1l_2\sin(\theta_1-\theta_2)-Rl_1\sin\theta_1}{l_2+R\cos\theta_2}\right) \end{bmatrix} \quad (1)$$

where g, θ, $\dot{\theta}$, l, $\dot{l}$ and l_0 represent gravitational acceleration (m/s^2), the leg angle (rad), the leg angular velocity (rad/s), the leg length (m), the leg velocity (m/s), and the slack length (m), respectively. The trailing leg and the leading leg at the double support gait phase are denoted by the subscripts '1' and '2'.

For each simulation used to integrate the differential equation, the model was initially positioned at the apex of the single support. As one possible initial condition that satisfies zero vertical speed (v_y) at the apex, such as, $v_y=\dot{l}_1\cos\theta_1-l_1\dot{\theta}_1\sin\theta_1=0$, we set θ_1 and $\dot{l}_1$ to be zero, and $\dot{\theta}_1$ and l_1 were obtained from the experimental data of the CoM at the apex. When the CoM is located at the position, where the tip of the unstretched imaginary leading leg (l_0) with a specific touchdown angle (θ_{td}) hits the ground, such that $l_1\cos\theta_1=l_0\cos\theta_{td}$, the single support phase was complete, and the double support phase began. The touchdown angle, defined as the angle of the leading leg with respect to the vertical, used for each simulation, was estimated from the gait trial per simulation. The double support continued until the spring of the trailing leg returned to its slack length. After a couple of steps of relatively large transient, the GRFs simulation data corresponding to the third to the fifth steps were compared with the empirical GRFs data (Fig. 3). To determine whether the 6th step and ensuing steps would be non-falling, repeated steps, we continued the simulation through 10 steps. We obtained the spring stiffness, k, and the damping constant, c, that minimized the least square error between the model-simulated GRFs and the data using a non-linear equation solver (fminsearch, MATLAB®). We did not explicitly match the CoM excursion, but because it was obtained from the integration of the GRFs (Donelan et al., 2002; Gard et al., 2004), it automatically fit by GRFs match. The model parameters used for the simulation were determined from the data or from the literature (Whittington and Thelen, 2009) and are shown in Table 1. The correlations between the effective leg stiffness obtained from the model simulation that best fit the GRFs data were compared with the vertical stiffness obtained from the force-displacement relationship (Lipfert et al., 2005; Rebula et al., 2009). Specifically, the vertical limb stiffness was calculated from the ratio of the vertical GRF change to the vertical CoM excursion during the single support (SS) phase (Fig. 5A). To perform a statistical analysis on the differences in the gait characteristics between the two groups, an independent t-test was used.

3. Results

The healthy older adult group showed significantly ($p<0.05$) slower natural and maximum gait speeds than the young group (Fig. 2A). The duration of both the single- and the double-support phase decreased with gait speed in a similar pattern for both groups (Fig. 2B,C), but slightly greater variations were observed for the older adult group. The model simulations reproduced the trajectories of the GRFs with a goodness of fit of $R^2=0.77\pm0.04$

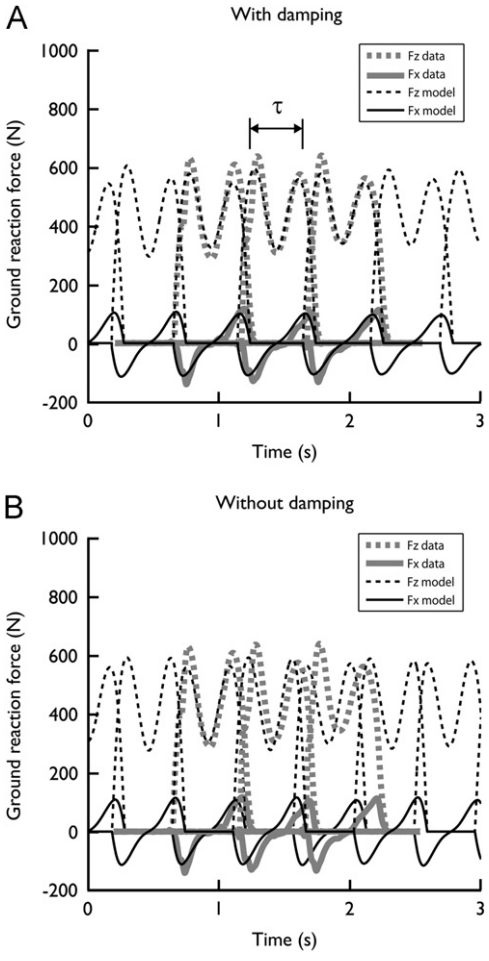

Fig. 3. The experimental (gray lines) and the model simulation (black lines) of GRFs data for trials at $v=1.36$ m/s. The stiffness and damping constant used for these simulations were 16.98 kN/m and 0.044, respectively. The simulations (A) with and (B) without the damper are presented. The solid and dotted lines indicate the horizontal (A–P) and vertical components of the GRFs, respectively.

and $R^2 = 0.77 \pm 0.03$ for the young and the older adult group, respectively (Fig. 3A). Although small in magnitude, the damping component of the model significantly increased the robustness of the fitting results (Fig. 3).

The stiffness of both age groups increased with speed ($p < 0.005$) (Fig. 4A). The damping ratios, though relatively small, demonstrated a significant correlation with the gait speed for both age groups ($r = 0.91$ and 0.84 for the young and the older adults, respectively) (Fig. 4B). There was a strong correlation between the vertical stiffness and the leg stiffness obtained from the data fitting using the compliant bipedal walking model (Fig. 5B).

4. Discussion

We found that spring-like leg dynamics during walking were consistently observed for both the young and the older adult subjects with greater variations in leg stiffness observed for the older adults (Fig. 4). Similar to many previous attempts to describe gait dynamics using stiffness parameters (Holt et al., 2003; Geyer et al., 2006; Whittington and Thelen, 2009; Kim and Park, 2011), the spring-like leg could successfully represent the CoM excursion (not shown) and the corresponding GRFs during

Table 1
The model parameters used for the simulation. Initial leg angular velocity, leg length, and touchdown angle were determined from the data and normalized by the subject's weight, height, and gravitational acceleration.

Model parameters	Subjectgroup	Range (or value)	
		Min.	Max.
Initial leg angle, θ_1	Young	0 (assumed)	
	Older adults	0 (assumed)	
Initial leg angular velocity, $\dot{\theta}_1$ (normalized)	Young	0.435	0.870
	Older adults	0.470	0.700
Initial leg length, l_1 (normalized)	Young	0.353	0.406
	Older adults	0.343	0.392
Initial leg length velocity, $\dot{l}_1$	Young	0 (assumed)	
	Older adults	0 (assumed)	
Touchdown angle, θ_{td} (rad)	Young	0.547	0.779
	Older adults	0.589	0.743
Slack length, l_0 (normalized)	Young	0.359	0.421
	Older adults	0.361	0.407
Radius of the curved foot, R	Young	0.3 m	
	Older adults	0.3 m	

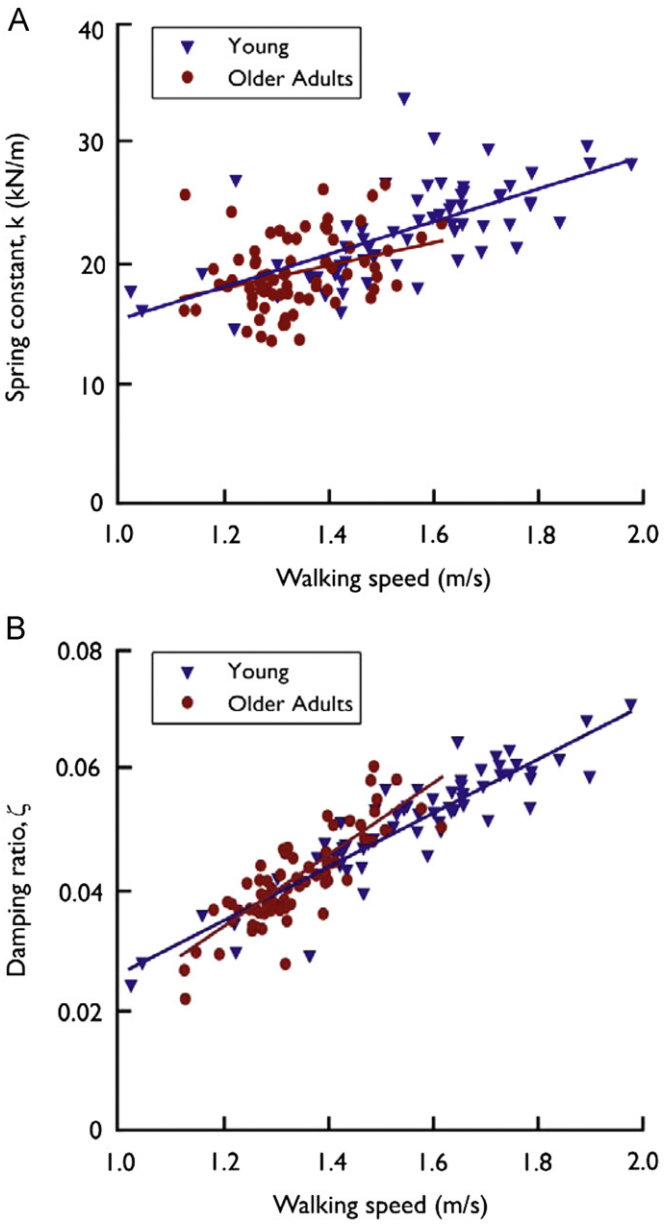

Fig. 4. (A) The spring constant, k, and (B) the damping ratio, ζ, (defined as) for all subjects are shown as a function of walking speed. Linear regression curves are shown as solid lines, and the corresponding regression parameters are listed in Table 2.

Table 2
Regression coefficients calculated for the gait parameters and the results of the statistical tests on the young and older adult subjects.

Regression equation (figure number in parenthesis)		Subject group	Slope A	Offset B	r (Pearson correlation coefficient)	p
D.S. duration (s)$=A/v+B$	(2B)	Young	0.125	0.015		
		Older adults	0.103	0.034		
S.S. duration (s)$=A/v+B$	(2C)	Young	0.324	0.155		
		Older adults	0.269	0.194		
Step length (m)$=Av+B$	(2D)	Young	0.105	0.513	0.65	1.11e−12
		Older adults	0.101	0.504	0.35	0.0004
k (kN/m)$=Av+B$	(4A)	Young	13.69	1.587	0.66	2.8e−9
		Older adults	9.533	6.441	0.32	0.006
$\zeta=Av+B$	(4B)	Young	0.045	−0.019	0.91	7.89e−26
		Older adults	0.061	−0.040	0.84	6.46e−20
k (kN/m)$=Ak_{vert}+B$	(5B)	Young	0.969	10.62	0.75	1.89e−11
		Older adults	0.585	13.60	0.60	7.61e−6

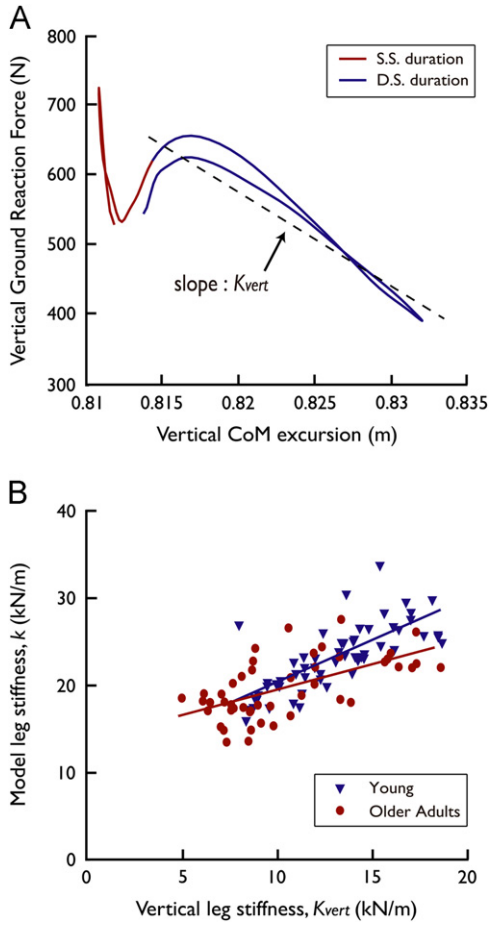

Fig. 5. (A) The definition of the vertical stiffness. The slope of the linear regression (dashed line) of the vertical GRF with respect to the vertical CoM excursion indicates the vertical stiffness of the single support phase. (B) The vertical stiffness as a function of the corresponding leg stiffness during the same gait trial. The solid lines indicate the linear regression.

several gait cycles reasonably well (Fig. 3A), which implies that the compliant leg bipedal model is a good candidate for describing the CoM dynamics during walking over a broad range of subject ages. Consistent with previous observations on increased joint stiffness or vertical stiffness with speed (Fonseca et al., 2001; Holt et al., 2003; Rebula et al., 2009), leg stiffness increased with gait speed (Fig. 4).

The possible benefits of springy dynamics may be related to the optimal energy (Holt et al., 1995; Kim and Park, 2011, 2012). A previous study by Kim and Park defined the optimal leg stiffness to be the one that gives maximum elastic energy stored in the springy stance leg during a single support phase and presumes that a closer match of the estimated leg stiffness to the optimal stiffness would be the best use of spring-like leg mechanics. To examine this presumption, the correlation between the leg stiffness and the mechanical work performed and/or metabolic cost should be further examined. It is important to note that the simulated steps did not come from a limit cycle. Because of the damping component in the model, there is small but consistent energy dissipation occurring that increases the discrepancy between the initial condition of the data and that of later simulation steps, including in the GRFs data. Therefore, we fit the data using the 3rd to 5th steps of model simulation after the few dominant transients are settled and prior to the accumulation of damping effects. Although the data fit was performed by non-limit cycles, the close match between the GRFs data and the simulation obtained from the initial conditions extracted from the data implies that the inclusion of the active component to compensate for the energy dissipation, such as by hip joint torque (Maus et al., 2010), may easily generate the limit cycle that fits the data.

Notably, the physiological interpretation of leg stiffness is presumed to be an integrative effect of the joint kinematics and the resistance of the joint muscle, and no single musculoskeletal parameter could be directly matched as a whole-leg stiffness in the current model (Holt et al., 1995,2003; Davis and DeLuca, 1996; Zeni and Higginson, 2009; Kim and Park, 2011). Although muscle mechanics could be well modeled using a compliance model (Hill, 1938; Martins et al., 1998), force generation through muscle contraction involves an active process (Murray et al., 1984; Winter and Yack, 1987; Rose, 2006) that could not be represented by a passive mechanical component of a spring in the present model or by joint stiffness, which represents the passive load-holding characteristics of the muscle (Holt et al., 2003) and is defined as the ratio of the ground reaction force change to the unit CoM movement averaged over a certain portion of the gait cycle. To quantify the contribution of the joint stiffness to the whole-leg stiffness presented in our model, a multi-segment dynamic simulation must be performed at the expense of model complexity and calculation costs, but even this model would be limited as a mechanical analysis because it does not consider the effect of muscle mechanics (Yen and Nagurka, 1987; Koopman et al., 1995; Ren et al., 2007). The force generation by the lower limb is achieved through a coordinated combination of joint flexors and extensors, which also determine the joint kinematics that determine the overall CoM excursion. Therefore, we assumed that the whole-leg stiffness characteristics would be determined by the joint stiffness, which is representative of the joint resistance in both active and passive muscle mechanics and does not require further musculoskeletal analysis of the joint mechanics during the gait (Neptune et al., 2008; Kim et al., 2012). Thus, the change in the leg stiffness could be achieved by changes in muscle activation and the joint environment, as reported in previous studies (Hunter and Kearney, 1982; Zhang et al., 1998; Garderner-Morse and Stokes, 2001; Holt et al., 2003; Zeni and Higginson, 2009). The degeneration of muscle performance with age would then be a possible explanation for the reduced maximum leg stiffness observed in the older adults (Fig. 4). Although muscle strength remains the same, the controllability of the muscle force and sensory feedback significantly deteriorates with age (Verrilo, 1980; Light, 1990; Peterka et al., 1990; Kang and Dingwell, 2008; Seidler et al., 2010), which could possibly explain the large variations of leg stiffness (Fig. 4) between the two groups.

Conflicts of interest

None.

Acknowledgments

This research was supported by the Happy tech. program through the National Research Foundation of Korea (NRF), funded by the Ministry of Education, Science and Technology (no. 2011-0020939). The authors thank Heewon Park, Keonyoung Oh, Chang Keun Jung and Sung Eun Ahn for their contributions to the data collection.

References

Alexander, R.M., 1976. Mechanics of bipedal locomotion. In: Davis, P.S. (Ed.), Perspectives in Experimental Biology, pp. 493–504.
Blickhan, R., 1989. The spring-mass model for running and hopping. Journal of Biomechanics 22, 1217–1227.

Davis, R.B., DeLuca, P.A., 1996. Gait characterization via dynamic joint stiffness. Gait and Posture 4, 224–231.
Dobbs, R.J., Charlett, A., Bowes, S.G., O'Neill, C.J.A., Weller, C., Hughes, J., Dobbs, S.M., 1993. Is this walk normal? Age and Ageing 22, 27–30.
Donelan, J.M., Kram, R., Kuo, A.D., 2002. Simultaneous positive and negative external mechanical work in human walking. Journal of Biomechanics 35, 117–124.
Elble, R.J., Sienko-Thomas, S., Higgins, C., Colliver, J., 1991. Stride-dependent changes in gait older people. Journal of Neurology 238, 1–5.
Eng, J.J., Winter, D.A., 1995. Kinetic analysis of lower limbs during walking: what information can be gained from a three-dimensional model? Journal of Biomechanics 28, 753–758.
Farley, C.T., Gonzalez, O., 1996. Leg stiffness and stride frequency in human running. Journal of Biomechanics 29, 181–186.
Fonseca, S.T., Holt, K.G., Saltzman, E., Fetters, L., 2001. A dynamic model of locomotion in spastic hemiplegic cerebral palsy: influence of walking speed. Clinical Biomechanics 16, 793–805.
Gard, S.A., Miff, S.C., Kuo, A.D., 2004. Comparison of kinematic and kinetic methods for computing the vertical motion of the body center of mass during walking. Human Movement Science 22, 597–610.
Garderner-Morse, M.G., Stokes, I.A.F., 2001. Trunk stiffness increases with steady-state effort. Journal of Biomechanics 34, 457–463.
Geyer, H., Seyfarth, A., Blickhan, R., 2006. Compliant leg behaviour explains basic dynamics of walking and running. Proceedings of the Royal Society Biological Sciences 273, 2861–2867.
Hill, A.V., 1938. The heat of shortening and the dynamic constant of muscle. Proceedings of the Royal Society Biological Sciences 126, 136–195.
Himann, J.E., Cunningham, D.A., Rechnitzer, P.A., Peterson, D.B., 1988. Age-related changes in speed of walking. Medical and Science in Sports and Exercise 20, 161–166.
Holt, K.G., Fonseca, S.T., LaFiandra, M.E., 2000. The dynamics of gait in children with spastic hemiplegic cerebral palsy: theoretical and clinical implications. Human Movement Science 19, 375–405.
Holt, K.G., Jeng, S.F., R., R., Hamill, J., 1995. Energetic cost and stability during human walking at the preferred stride frequency. Journal of Motor Behavior 27, 164–178.
Holt, K.G., Wagenaar, R.C., LaFiandra, M.E., Kubo, M., Obusek, J.P., 2003. Increased musculoskeletal stiffness during load carriage at increasing walking speeds maintains constant vertical excursion of the body center of mass. Journal of Biomechanics 36, 465–471.
Hunter, I.W., Kearney, R.E., 1982. Dynamics of human ankle stiffness: variation with mean ankle torque. Journal of Biomechanics 15, 747–752.
Imms, F.J., Edholm, O.G., 1981. Studies of gait and mobility in the elderly. Age and Ageing 10, 147–156.
Kang, H.G., Dingwell, J.B., 2008. Separating the effects of age and walking speed on gait variability. Gait and Posture 27, 572–577.
Kim, K., Kim, Y.H., Lee, S., 2012. General computational model for human musculoskeletal system of spine. Journal of Applied Mathematics 2012, 8.
Kim, S., Park, S., 2011. Leg stiffness increases with speed to modulate gait frequency and propulsion energy. Journal of Biomechanics 44, 1253–1258.
Kim, S., Park, S., 2012. The oscillatory behavior of the CoM facilitates mechanical energy balance between push-off and heel strike. Journal of Biomechanics 45, 326–333.
Koopman, B., Grootenboer, H.J., de Jongh, H.J., 1995. An inverse dynamics model for the analysis, reconstruction and prediction of bipedal walking. Journal of Biomechanics 28, 1369–1376.
Larish, D.D., Martin, P.E., Mungiole, M., 1988. Characteristics of gait in the healthy old. Annals of the New York Academy of Sciences, 18–32.
Lark, S.D., Buckley, J.G., Bennett, S., Jones, D., Sargeant, A.J., 2003. Joint torques and dynamic joint stiffness in elderly and young men during stepping down. Clinical Biomechanics 18, 848–855.
Light, K.E., 1990. Information processing for motor performance in aging adults. Physical Therapy 70, 820–826.
Lipfert, S., Seyfarth, A., Blickhan, R., 2005. Leg stiffness in walking and running. In ASB 29th Annual Meeting.
Martins, J.A.C., Pires, E.B., Dinis, P.B., 1998. A numerical model of passive and active behavior of skeletal muscles. Computer Methods in Applied Mechanics and Engineering 151, 419–433.
Maus, H.M., Lipfert, S., Gross, M., Rummel, J., Seyfarth, A., 2010. Upright human gait did not provide a major mechanical challenge for our ancestors. Nature Communications 1, 70.
McMahon, T.A., Cheng, G., 1990. The mechanism of running: how does stiffness couple with speed? Journal of Biomechanics 23, 65–78.
Mochon, S., McMahon, T.A., 1980. Ballistic walking. Journal of Biomechanics 13, 49–57.
Murray, M.P., Kory, R.C., Clarkson, B.H., 1969. Walking patterns in healthy old men. Journal of Gerontology 24, 169–178.
Murray, M.P., Mollinger, L.A., Gardner, G.M., Sepic, S.B., 1984. Kinematic and EMG patterns during slow, free, and fast walking. Journal of Orthopaedic Research 2, 272–280.
Neptune, R.R., Sasaki, K., Kautz, S.A., 2008. The effect of walking speed on muscle function and mechanical energetics. Gait and Posture 28, 135–143.
Peterka, R.J., Black, F.O., Schoenhoff, M.B., 1990. Age-related changes in human vestibulo-ocular reflexes: sinusoidal rotation and caloric test. Journal of Vestibular Research 1, 49–59.
Rebula, J.R., O'Connor, S.M., Kuo, A.D., 2009. Human walking and running: it's all in the redirection. In Dynamic Walking.
Ren, L., Jones, R.K., Howard, D., 2007. Predictive modelling of human walking over a complete gait cycle. Journal of Biomechanics 40, 1567–1574.
Rose, J., Gamble, J.G., 2006. Human Walking, third ed. Lippincott Williams & Wilkins, Philadelphia, PA, pp. 53–76.
Seidler, R.D., Bernard, J.A., Burutolu, T.B., Fling, B.W., Gordon, M.T., Gwin, J.T., Kwak, Y., Lipps, D.B., 2010. Motor control and aging: Links to age-related brain structural, functional, and biomechemical effects. Neuroscience and Biobehavioral Reviews 34, 721–733.
Srinivasan, M., Ruina, A., 2006. Computer optimization of a minimal biped model discovers walking and running. Nature 439, 72–75.
Verrilo, R.T., 1980. Age related changes in the sensitivity to vibration. Journal of Gerontology 35, 185–193.
Wall, J.C., Hogan, D.B., Turnbull, G.I., Fox, R.A., 1991. The kinematics of idiopatic gait disorder. A comparison with healthy young and elderly females. Scandinavian Journal of Rehabilitaition Medicine 23, 159–164.
Whittington, B.A., Thelen, D.G., 2009. A simple mass-spring model with roller feet can induce the ground reactions observed in human walking. Journal of Biomechanics, 131.
Winter, D.A., 1991. The Biomechanics and Motor Control of Human Gait: Normal, Elderly, and Pathological. University of Waterloo Press, Waterloo.
Winter, D.A., Yack, H.J., 1987. EMG profiles during normal human walking: stride-to-stride and inter-subject variability. Electroencephalography and Clinical Neurophysiology 67, 402–411.
Winter, D.A., Patla, A.E., Frank, J.S., Walt, S.E., 1990. Biomechanical walking pattern changes in the fit and healthy elderly. Physical Therapy 70, 340–347.
Yen, V., Nagurka, M.L., 1987. Suboptimal trajectory planning of a fivelink human locomotion model. In ASME Winter Annual Meeting.
Yeom, J., Park, S., 2011. A gravitational impulse model predicts collision impulse and mechanical work during a step-to-step transition. Journal of Biomechanics 44, 59–67.
Zeni, J.A., Higginson, J.S., 2009. Dynamic knee joint stiffness in subjects with a progressive increase in severity of knee osteoarthritis. Clinical Biomechanics 24, 366–371.
Zhang, L., Nuber, G., Butler, J., Bowen, M., Rymer, W.Z., 1998. In vivo human knee joint dynamic properties as functions of muscle contraction and joint position. Journal of Biomechanics 31, 71–76.